

Classification of productive profile using brain signals: Deep learning and neuroscience meets the mining industry

1st Ana C. Q. Siravenha
Federal University of Pará
Federal University of Pará
Belém, Brazil
siravenha@ufpa.br

2nd Walisson C. Gomes
Vale Institute of Technology
Vale Institute of Technology
Belém, Brazil
walissoncardosogomes@gmail.com

3rd Renan A. Tourinho
Vale S/A
Vale S/A
Canaã dos Carajás, Brazil
renan.tourinho@vale.com

4th Sergio Viademonte
Vale Institute of Technology
Vale Institute of Technology
Belém, Brazil
sergio.Viademonte@itv.org

5th Bruno D. Gomes
Federal University of Pará
Federal University of Pará
Belém, Brazil
bruno.gomes@pq.itv.org

Abstract—Classification of electroencephalography (EEG) signals is a complex task. EEG is a non-stationary time process with low signal to noise ratio. Among many methods used for EEG classification, those based on Deep Learning (DL) have been relatively successful in providing high classification accuracies. In the present study we aimed at classify resting state EEGs measured from workers of a mining complex. Just after the EEG has been collected, the workers undergone training in a 4D virtual reality simulator that emulates the iron ore excavation from which parameters related to their performance were analyzed by the technical staff who classified the workers into four groups based on their productivity. Two convolutional neural networks (ConvNets) were then used to classify the workers EEG bases on the same productivity label provided by the technical staff. The neural data was used in three configurations in order to evaluate the amount of data required for a high accuracy classification. Isolated, the channel T5 achieved 83% of accuracy, the subtraction of channels P3 and Pz achieved 99% and using all channels simultaneously was 99.40% assertive. This study provides results that add to the recent literature showing that even simple DL architectures are able to handle complex time series such as the EEG. In addition, it pin points an application in industry with vast possibilities of expansion.

Keywords: electroencephalography, machine learning, convolutional neural networks, mining industry, virtual reality environment

This research is financed by the Instituto de Tecnologia Vale, the Coordination for the Improvement of Higher Education Personnel (CAPES) at process 88887.141251/2017-00, and by the National Council for Scientific and Technological Development (CNPq) at calls ChMCTI/CNPq/VALE-ITV (443304/2015-7), CNPq/ITV 2018 (402764/2018-8) and DT-2018 (315462/2018-3).

I. INTRODUCTION

The electroencephalography (EEG) is an electrophysiological monitoring method that is used to record the electrical activity of the brain via scalp electrodes. It is widely used for application in the diagnosis of neurological and mental health disorders, monitoring of mental states, and in brain-computer interface systems [1]–[3]. It is a less complex alternative to both resonance and tomography recordings. It is also much cheaper and provide high time resolution. Typically, when using EEG in basic or applied cognitive research, one might want to identify a pattern of cortical activity while subjects perform some task of interest. These studies aim to identify some condition or mental state while the subjects engage in a specific routine under a controlled environment. In contrast, the resting state EEG is the EEG elicited in the absence of task routines or stimulation. In general, in this scenario, the subject lies quietly with closed or opened eyes. The analysis of this state is supposed to provide the default configuration of the brain which may offer a better signal-to-noise ratio than the task-based experiments and allows for the study of different cortical systems [4].

In the present study a task free EEG recording was performed before and after a scenario the simulated a operational routine commonly performed in a mining industry. The EEG elicited at these conditions is commonly referred to as resting state EEG and despite not being evoked by stimuli which the parameters are known, it can provide valuable information about how the default functional brain network behaves in normal [5], [6] as well as altered brain function caused by diseases [7]. It can also predict attentional levels and mental fatigue [8]–[10], characterize disorders of consciousness [11] and even clearly indicate a signature of hemispatial

neglect [12].

Despite the success of EEG at probing cortical activity, due to its inherent low signal-to-noise ratio, poor spatial resolution plus its non-linear and non-stationary nature, most of the EEG studies show that frequently a long run of pre- and post-processing steps have to be taken before stating any conclusion. Because of that there has been always a quest for methods that might account for these natural EEG complexities. The current AI revolution based on neural networks has provided efficient algorithms based on deep learning that are capable of extracting informative features from complex and multidimensional data with minimum or none pre-processing steps. This original bypassing of steps in data processing has already been explored using EEG as input data to various neural networks architectures and training paradigms and with promising results [13], [14]. In the present study we aimed at classify the EEG from workers of a mining complex just before they are undergo training at a 4D VR simulator. The EEG was the used as input to a ConvNet for classification in a supervised learning pipeline. The labels were three levels of productivity and were provided by the technical staff after analyzing the workers performance in the VR simulator. That is, the evaluation of the behavioral data was used as the ground truth for the workers productivity performance.

The raw EEG was separated in three sets comprising three input databases for the CNN. The aim was to identify the classes according to the productive profiles. In the following sections we detail the experiment and the model used to cluster the behavioral data (Sections II-A and II-C). The EEG pre-processing, datasets definition as well as details of the CNN used, are discussed in sessions II-D to II-F. The results and the discussion are the next two following sessions, III and IV.

All procedures performed in the present study were in according with the Helsinki Protocol and were approved by the Research Ethic Committee of the Universidade Federal do Pará, Brazil (Protocol #3601269).

II. MATERIALS AND METHODS

A. Protocol of simulated iron ore excavation

During this study, 25 healthy male subjects aging from 26 to 53 years old performed the protocol of simulation of excavation pictured in the Figure 1. The subjects are experienced workers in mining industry and the excavation simulator is one of the gadgets used to train and improve their skills.

The used simulated environment is the EF144 conversion kit for Caterpillar 7495 rope shovels from Immersive Technologies. It simulates the real conditions in an actual rope shovel cab, for this, the kit includes a complete replica cab of the Caterpillar 7495 Rope Shovel excavator, with fully functional controls and instrumentation sourced directly from Caterpillar, and three large displays to mimic a panoramic field-of-view to the operator.

The protocol takes 91 minutes plus the time required to the system calibration which varies according to several factors. It begins with the collection of EEG during three minutes

of resting state with eyes opened, i.e., a period in which are discouraged voluntary movements, while stay comfortably seated in front of a white screen in a silent room with controlled luminosity.

Following, the subject proceed 15 minutes of adaptation to the simulated scenario. Through the sessions the virtual scenario was kept the same, thus the mining bench height, the ore granularity and the initial position were equal to all subjects. The EEG data of this period was ignored.

After the adaptation, an uninterrupted session of 60 minutes occurs, with EEG being captured. The subjects were instructed to avoid verbalization, and act naturally, aiming the highest production rate and lowest errors rate.

At the end of the 60 minutes, a new three minutes session of resting EEG was recorded.

B. Technical data from ore excavation

The simulation environment allows the monitoring of every movement during the cycles. The entire session consisted of many excavation cycles which are a sequence of tasks the subject must repeat. First, they have to use the bucket to excavate the ore, then perform a loaded spin to the location of the mobile crusher, and finally do an empty spin back to the location of the ore.

Each of these movements are monitored by technical indicators that describes how the individual operates the simulator and where the various operational measures are taken from. Of all indicators, 12 can be listed as being the most important to indicate the subject's performance. The productivity of a single cycle is the measure of the cycle time (excavation time, loaded-spin time, and empty-spin time) measured in seconds along with the unloaded bulk measured in tons. Moreover, the subject's final productivity for the session is the average of all the single-cycle productivity.

C. Operational classes definition

As stated before, the main goal of the work described in this paper is to classify the workers performance using their recorded resting EEG data. In order to do that, the behavioral or the operational label of each subject is necessary.

The objective of the operational classifier is to produce a data partitioning so that it is possible to discriminate the average productivity in classes. The K-means algorithm was employed for this purpose. However, since the number of operators is limited, a non-parametric cluster validity index called Mutual Equidistant-scattering Criterion (MEC) is used to better determine the number of clusters [15].

The MEC index is a hyperparameter-free technique based on the mutual equidistant dispersion between data within clusters, for fine-tuning the number of clusters (K). It returns the partitioning configuration with smallest inter-cluster separation and largest intra-cluster homogeneity. In our data, the algorithm suggested a $K = 4$. Thus, we ran the K-means algorithm to partition the samples into four groups, named "A", "B", "C" and "D", in decreasing order of average productivity. In the

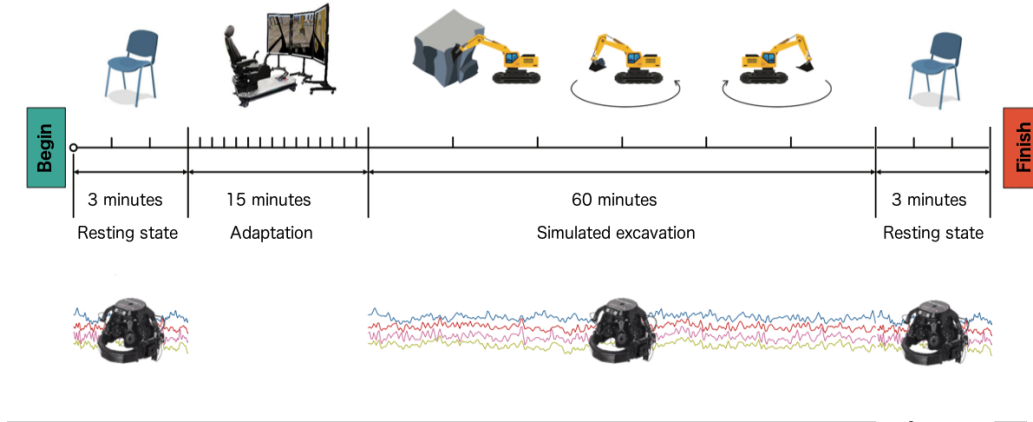


Fig. 1: Protocol of EEG collection during the activity of simulated ore excavation.

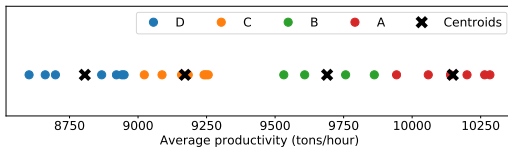


Fig. 2: Distribution of subjects across clusters defined by the K -means algorithm.

Figure 2 is illustrated the partitioning of data, including the position of centroids determined by the clustering method.

Centroids are the location of the center of each cluster which aggregates the samples with similarities. From the centroids presented here, new future data can be attributed and, thus, expand the application of this proposal.

In the Table I are presented the classes and their ranges defined by the K -means and the proportion of the distribution of subjects through the classes. \overline{AP} denotes a measure of average productivity calculated from a single simulation session.

TABLE I: Grouping details.

Class	Range of average productivity	Proportion of subjects
<i>A</i>	$\overline{AP} \geq 9919.05$	0.29
<i>B</i>	$9430.35 \leq \overline{AP} < 9919.05$	0.29
<i>C</i>	$8988.41 \leq \overline{AP} < 9430.35$	0.17
<i>D</i>	$\overline{AP} < 8988.41$	0.25

D. EEG data

The EEG data were collected using the BrainMaster 24D headset. The headset had 21 electrodes positioned according to the 10-20 system [16]. EEG was recorded at a sampling rate of 300Hz.

All the data were acquired using channel Pz as reference. A re-referencing was implemented for the linked ears channels, A1 and A2. This referencing was preferred due to excess noise in some recordings.

After re-referencing, the data were double filtered. First, by a Butterworth filter from 1 to 100Hz, bounding the spectrum to the frequency range of interest. Then, a reject band filter was applied at frequencies 50Hz and 60Hz to filter out the power line noise interference. The recordings were then segmented in trials of one second, each with 300 data points. As there was no behavioral markers to time stamp the recordings we deliberately choose the trials time-window to correspond to the lower bound of band-pass filter. The pre-processing was performed using the Matlab toolbox FieldTrip [17].

E. EEG datasets

The EEG data allows a large variety of arrangements for data processing. During this study three assumptions were tested regarding the number of channels (electrodes) necessary to form the samples used in classification: 1. using the 19 available channels, 2. using each of the 19 channels individually, and 3. using the subtraction of pairs of channels.

The resting state sessions, nominally containing three minutes (or 180 seconds), actually lasted a few seconds beyond it. Thus, for simplicity, it was adopted for all subjects, the first 200 seconds to represent one session of resting state. This means that the amount of samples in every tested dataset was equal to 5000. For training, validation and testing purposes, the samples were split in proportion of 70%, 20% and 10%, respectively.

The datasets are composed as follows:

- 1) **All available data (AD)**: samples were a 19×300 matrix, where 19 is the number of available channels, 300 is the number of data points in one second.
- 2) **Individually channels (IC_N)**: with N meaning a given channel. There were then 19 datasets for this configuration, each one of size $1 \times 300 \times 1$, corresponding to one second sampled.
- 3) **Channel subtraction (CS_O)**: The O represents every 342 possible subtraction between two channels. The samples dimension was as in IC_N.

F. Applied Convolutional Neural Network Models

From the technical data perspective is possible to split the workers in different groups of productivity from a clustering method such as the K-means. This study aims to find if, from the cognitive data perspective taken from the resting state, it is possible to identify in which group of productivity a worker fits in.

It is important to note that this assumption has a strict relation between the resting state data and the session of excavation immediately taken. Therefore, even if there is more than one session for a single worker, it will be treated as independent sessions. It is also acceptable that they are in different productive groups.

From several models of machine learning, stand out the convolution neural networks (CNN). It is an algorithm able to learn from an input signal, assigning importance to features in order to distinguish objects according to categories previously defined. It is able to successfully capture spatial and temporal dependencies by using convolutional filters. These networks do not request the feature extraction step which is an important characteristic of these models, among others [18], [19].

The CNN architecture is a sequence of layers with convolutional filters, normalization, regularization and pooling components followed by fully-connected layers. The arrangement of the layers is empirically defined as well as the parameters involved in the model training.

In the Figure 3 are presented the models proposed to classify the EEG data. The main difference between them is the input layer. Three types of datasets were composed and two architectures were tested. The one one-dimensional network (1D-CNN - Fig. 3a) is proposed to handle the datasets including the single channels and those datasets with channel subtractions, IC_N and CS_O , respectively. The two-dimensional model (2D-CNN - Fig. 3b) is used to deal with the dataset in which all channels are used in the same sample (AD).

Both architectures are quite simple and not very deep. They contain between four and five convolutional layers followed by normalization and regularization. Dropout layers range from 10% to 20%. The 2D-CNN has smaller filter sizes in its convolutional layers than those in the 1D-CNN, which gradually decrease from 1×50 to 1×10 . This architecture has one additional fully-connected layer of 128 neurons. Both models ends with a fully-connected layer of four neurons (corresponding to the number of classes), and the *softmax* function to map the non-normalized output to a probability distribution over the four predicted output classes.

III. RESULTS

The classification of biomedical signals has a large field of applications, from diagnostic to mental states characterization. This work proposes the identification of stimulus free scalp electrical signals measured just before the session of mining digging as productivity indicators.

Several tests to determine the best classifier model to distinguish the groups according the k-means grouping were

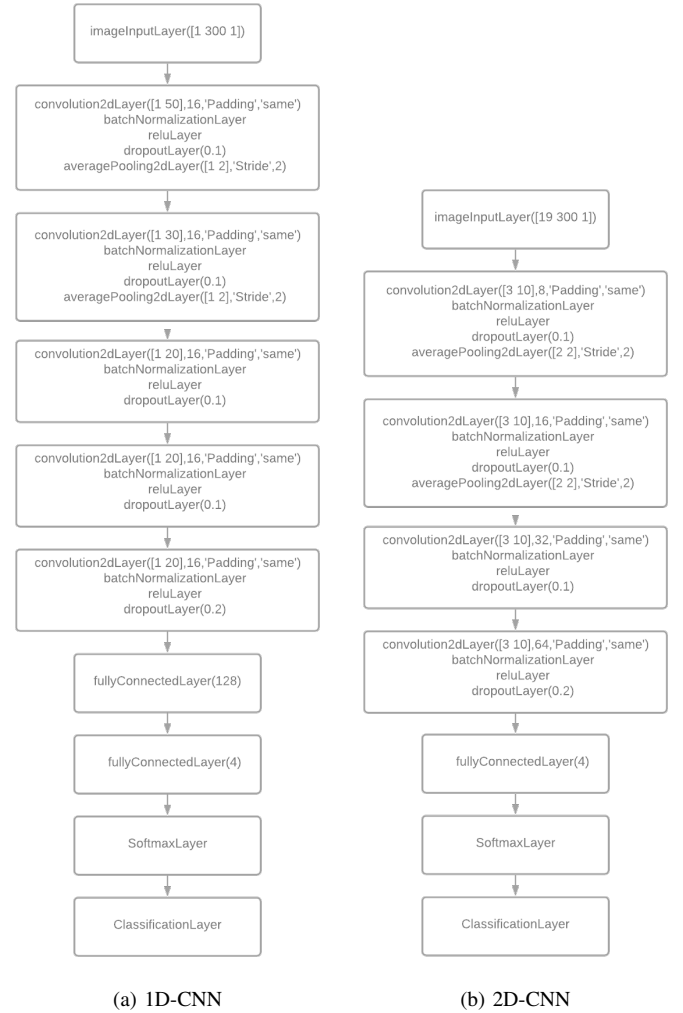


Fig. 3: Diagrams of the convolutional neural network used for EEG classification.

proceeded. The tests that achieved better performances are discussed in this document, and presented in Table II. According this table, the best classification performance was obtained with the AD dataset, which contains all data (19 channels), followed by the CS_{P3-Pz} dataset, which contains the subtraction between channels P3 and Pz. The dataset IC_{T5} , which contains data obtained from channel T5, showed a smaller accuracy measure, of 83% correctly classified instances. Those results are discussed in detail in the following paragraphs.

The mini-batch size of all tests was equal to 256, the maximum number of epochs was 100 and learning rate of $1e-3$. At every 13 iterations the validation was applied, and the absence of significant variation in the model's performance after 15 validations interrupted the training, avoiding overtraining. The optimization algorithm was the well know stochastic gradient descent with momentum (SGDM) [20].

The promising results indicate the feasibility of identifying an operator's productive state given his pre-activity mental state, even at rest. In Tables III and V are presented the test's

TABLE II: Test accuracy of the different models for EEG classification.

Dataset	Test accuracy (%)
<i>AD</i>	99.40
<i>IC_{T5}</i>	83.00
<i>CS_{P3-Pz}</i>	99.00

TABLE III: Confusion matrix of test of *AD* model.

Group	A	B	C	D
A	100	0	0	0
B	1	76	1	1
C	0	0	149	0
D	0	0	0	172

confusion matrices of the described models.

From the 500 samples, three were wrongly assigned by the most accurate model, *AD*, in Table III, while the double of samples was misclassified by the *CS_{P3-Pz}* model (Table V).

In general, the class 'B' was the most difficult to be distinguished from the others. Using the model *IC_{T5}*, Table V, 20 samples of this class were miss classified, in particular to the class 'C'. In fact, the gap between the amount of ore dug from the most productive group ('A') and the least produced ('D') is approximately 2,000 tons per hour, which in practical terms is a subtle difference; all subjects are at a satisfactory productive level.

IV. DISCUSSION

Resting brain activity has been correlated with personal traits, such as neurological disorder, and with event-based applications [21]. In this work, we studied the potential use of EEG resting activity taken immediately before the task of mining ore simulation. The classification task aimed to differ samples of EEG allocated into four groups according the productivity efficiency of 25 volunteers, clustered by the k-means algorithm.

The accuracy measures achieved during the tests were higher than the theoretical chance level, 25%. It is well know that this value consider an infinite number of samples and it is very common the achievement of this threshold by

TABLE IV: Confusion matrix of test of *IC_{T5}*.

Group	A	B	C	D
A	81	5	7	25
B	2	49	11	7
C	1	9	133	6
D	1	4	7	152

TABLE V: Confusion matrix of model tested with *CS_{P3-Pz}* samples.

Group	A	B	C	D
A	122	0	1	0
B	0	81	0	1
C	0	0	127	0
D	1	0	2	165

chance. Consulting a look-up table available for Combrison and Jerbi [22], can be verified that most of the tests reliably exceed the chance level. In Tables VI and VII the ranges of accuracy of each channel subtraction and isolated channel tested during this work are shown, respectively.

From the pairs in Table VI, 59 provided accuracy rates higher than 70%. 33.9% of the channels in these pairs came from the frontal and frontopolar region of brain (21.18% and 12.72%, respectively). At least one parietal channel composed 20.33% of the subtraction pairs, while 17.79% of the channels came from the temporal or central regions, each. In comparison to the pairs with accuracy lower than 70% the distribution of channels follows approximately the same behavior, but with a higher proportion of parietal channels in the most accurate group.

The subtraction of channels is a strategy commonly used to reduce noise or artifacts [23], [24]. Similarly, when subtracting two channels, the common noise between the channels is reduced, improving the overall quality of the signal.

The higher performance achieved by the subtraction of two parietal electrodes is interesting when considering the context of the activity. It is known that the parietal region is mainly responsible for forming of motor intention and interpreting the somatosensory signals, such as movement coordination and visual perception [25], [26]. Thus, there is the assumption that the briefing made before the beginning of the experiment can induce a mental arrangement in the volunteers, who are already used to the virtual environment of the activity.

In the Table VII is shown that channels located at the left side of brain are the majority of those with 70% or higher accuracy. The frontal or frontopolar channels were, in general, less accurate than the others. Temporal lobe is classically related to perception and recognition of auditory stimuli, speech and also semantic memory [27]. Semantic memory refers to a portion of long-term memory of things or objectives that are common knowledge, such as the experiment.

The subjects involved in this experiment are experienced employees both in real as in simulated environments. However, several factors can influence the operation in simulated experiments, such as, the reticence about the technology of virtual reality. It is not uncommon experience some physical discomforts (dizziness or nausea, for example) in this type of environment due the difficult of the brain to interpret the projections [28].

By analyzing the statistical test of Wilcoxon of groups we can observe two significant differences between groups medians, A with relation to B and C, and D to B and C. The Wilcoxon test is a nonparametric test for equality of population locations (medians). The p-value observes the null hypothesis, when two populations enclose identical distribution functions, or the alternative hypothesis, when two distributions differ regarding the medians. In the Table VIII is shown that the group A does not differ significantly from the group D. Also, the group B and C are the closest group among groups.

The similarity p-value pointed by the Wilcoxon test does not consider the temporal relation of the EEG data, also this

TABLE VI: Ranges of accuracy of the 342 pairs of channels subtraction of CS_O dataset.

Range of accuracy (%)	Pairs
]30-40]	P3-T4, F3-F7, C3-P4, F3-O2, F3-T4, Cz-T6, F3-T6, C3-Fz, T3-F7, F3-F4, F4-T5, C3-T4, P3-C3, C3-Cz, T3-T4, P3-Cz, Fz-P4, F4-T4, P4-F7, P4-T3
]40-50]	F3-O2, Fp2-Pz, F4-Cz, P4-T5, F7-Pz, T3-T4, F8-Pz, Fp1-Pz, F3-F4, F7-F8, F3-T5, F4-P4, P4-T5, C4-T3, P4-T4, Cz-F7, O2-T6, F7-Pz, F3-Pz, P3-F4, P3-F7, F3-F8, C4-P4, Cz-O2, Fp1-T4, C3-F7, F3-P4, Fz-F7, C4-F7, Cz-T3, F4-Cz, O1-O2, Fz-T4, F8-Pz, Cz-T5, Cz-O1, O2-T4, F7-T4, P3-T3, C3-F3, C3-O1, Fp1-Pz, C3-F4, C3-O2, C3-T6, F4-T3, F4-T6, P4-O2, T5-T6, Fz-O2, F4-O2, O1-T4, P3-F3, P3-O2, C4-T6, T3-O2, P4-F8, Fp2-Pz, O2-F7, F8-T6, C3-T3, F3-Cz, Fp2-T6, T5-O1, T5-O2, Fz-T3, P4-Cz, P4-T6, Fp1-F7, P3-Fz, F3-T3, F3-O1, T5-T4, F7-F8, C3-C4, F3-C4, Fz-C4, F4-C4, C4-T4, Fp1-F8, Fp2-O1, Fp2-F7, Fp2-F8, F3-Fp1, Cz-T4, F4-F7, C4-O2, T3-T6, P3-P4, C3-Fp2, C3-F8, Cz-F8, O1-F8, F8-T4, T6-T4, Fz-O, T5-F8, F4-O1, O2-F8
]50-60]	Fp1-F8, Fp1-Fp2, Cz-T5, C3-C4, Fp2-F8, F3-T6, T5-O1, Cz-O1, P4-F7, T3-F8, O2-F7, C4-O2, F3-T3, F3-T5, P4-Cz, Fz-P4, Fp2-O2, F3-F8, F4-T4, P4-F8, Cz-T6, Fp2-F7, O2-F8, C3-F8, C3-F7, C4-T5, F8-T6, P3-T4, P4-T6, F3-F7, F3-Pz, Fz-Cz, F4-F7, Fp1-T6, C3-F4, P4-Fp1, P4-Fp2, F4-T3, C4-Cz, Fz-T6, C4-T5, Fz-F4, C4-O1, Fp1-Fp2, T3-F8, O1-F7, C4-F8, Fz-Cz, Fz-T5, C4-Cz, O1-T6, P3-T6, F4-F8, P3-F8, P4-O1, T3-T5, T5-F7, C3-Fp1, F3-Fp2, Fp1-O1, Fp2-O2, F4-Fp2, Fp2-T5, P4-Fp2, C4-Fp1, P3-C4, C3-T5, Fp1-T5, P3-O1, Fp2-T3, T3-O1, F4-Fp1, Fp1-T3
]60-70]	P3-P4, O2-T6, Fz-O1, C4-T4, P4-T3, Cz-T4, C3-T4, Fp1-T4, C4-F7, T5-T4, Cz-T3, O1-O2, F4-F8, P3-O2, F3-P4, T5-F8, P3-C3, C4-T3, F7-T6, Fp1-F7, C3-T6, P3-F4, F3-O1, P3-C4, F4-T5, T5-O2, P3-T6, Cz-F8, Fz-O2, Fp1-O1, T5-F7, F3-Fp2, T4-Pz, C3-O2, P3-Cz, P4-T4, Fp2-O1, F4-P4, Fz-C4, P3-Fz, F3-Fz, Fp1-T5, F3-T4, F4-C4, Cz-O2, Cz-F7, T3-O2, F7-T4, F4-O1, F8-T4, Fz-T6, P3-Fp1, C3-Fp1, O1-F8, C4-T6, F3-Fp1, F4-T6, P4-O1, T3-T5, T3-F7, Fp2-T5, T3-T6, O1-T4, P3-T5, Fp1-O2, T3-Pz, Cz-Fp2, Cz-Fp1, F7-T6, P3-Fp1, P4-Fp1, Fz-Fp1, F3-Fz, Fp2-T4, C3-Pz, Fp1-T6, O1-Pz, C4-Fp2, T6-Pz, T5-Pz
]70-80]	Fp1-T3, Fp2-T6, C3-Fp2, F4-Pz, T5-T6, O1-T6, P3-T3, Fp1-O2, C3-T5, Fz-T3, T3-Pz, C4-Fp1, C3-Fz, T6-T4, C3-T3, F3-Cz, P4-Pz, P3-F8, C4-O1, Cz-Fp2, Fz-T5, P3-F3, P3-F7, Fz-F7, C3-Cz, Fp2-T3, Fp2-T4, O2-T4, P4-O2, Cz-Fp1, F4-Fp1, C4-F8, Fz-T4, O1-F7, P3-T5, T3-O1, C3-F3, C4-Fp2, O1-Pz, Fz-F8, T6-Pz, F4-O2, C3-P4, Fz-F4, F4-Fp2, Fz-Fp2, T4-Pz, Fz-F8, F4-Pz, P3-Fp2, P3-Pz, C4-Pz
]80-90]	P3-Fp2, Fz-Pz, P3-O1, C4-Pz, F3-C4, C3-O1, T5-Pz, C4-P4, C3-Pz, Fz-Fp2, O2-Pz, Cz-Pz, P4-Pz, Fz-Pz, Cz-Pz
>90	Fz-Fp1, P3-Pz, O2-Pz

TABLE VII: Ranges of accuracy of the IC_O dataset.

Range of accuracy (%)	Channels
]40-50]	Pz, Fp2, F7
]50-60]	F8, Fp1, F3, Fz, P4
]60-70]	C3, T4, O2, T3, T6, F4
]70-80]	P3, C4, O1, Cz
]80-90]	T5

TABLE VIII: Wilcoxon rank sum test for equal medians.

Groups	p-value
A, B	< 0.01
A, C	< 0.01
A, D	0.5862
B, C	0.6498
B, D	< 0.01
C, D	< 0.01

test assumes a normal distribution of the signals and may not reflect the complexity of the signal presented.

Entropy-based measures are commonly employed to characterize time series, such as the EEG, since they can quantify the complexity of them [29]. In particular, the method of permutation entropy (PE), proposed by Bandt and Pompe [30], measures the irregularity of non-stationary time series. Their proposal considers the relations between the values of a time series rather than the values themselves in a simple, fast and robust way.

PE values ranges from zero to one, where the largest value means that all permutations have an equal probability, indicating that the time series is highly irregular; the opposite is true, indicating the presence of regular patterns over the signal. In the Figure 4a and in the Figure 4d are presented the PE of the average EEG values of each group. Since this study

uses an EEG recording not too long, the order is preferable not large, thus we calculate the PE with order $n = 3$, window of size 30 and one sample windows shift, culminating in 168 values of permutations.

By analyzing the differences between the permutation entropy of channels between groups we found that 17 of 19 channels present some similarity. P4 and F8 are the two significantly different in all tests made, and the two temporal right-positioned electrode, T6 ad T4, failed the test in five and four tests, respectively.

The channel T5, the one with the highest accuracy among the IC_O datasets, presented similarity between groups B and C. All the three comparisons with group A identified significant similarities in the channels T6 and T4; two of the tests identified the correspondence in channels O2, P3 and F4. The six channels with accuracy between 60% and 70% failed in 17 of 36 tests of similarity.

V. CONCLUSION

In the present study we have shown a very high accuracy for the classification of task free EEG signals using convolutional neural networks. The accuracy was obtained with a classical ConvNet architecture which demonstrate the feasibility of DL architectures based on filters convolution for the classification of time series as complex as the EEG. Obtaining this result was remarkable when two things are taken into account: i. The EEG used was a task free scalp recording. That is, it was not recorded during training in the VR simulator. ii. The productivity label used to train the ConvNet in a supervised learning pipeline was not adapted in any level to specifically extract meaningful physiological information. That is, the EEG was recorded before and after a routine training of workers in the

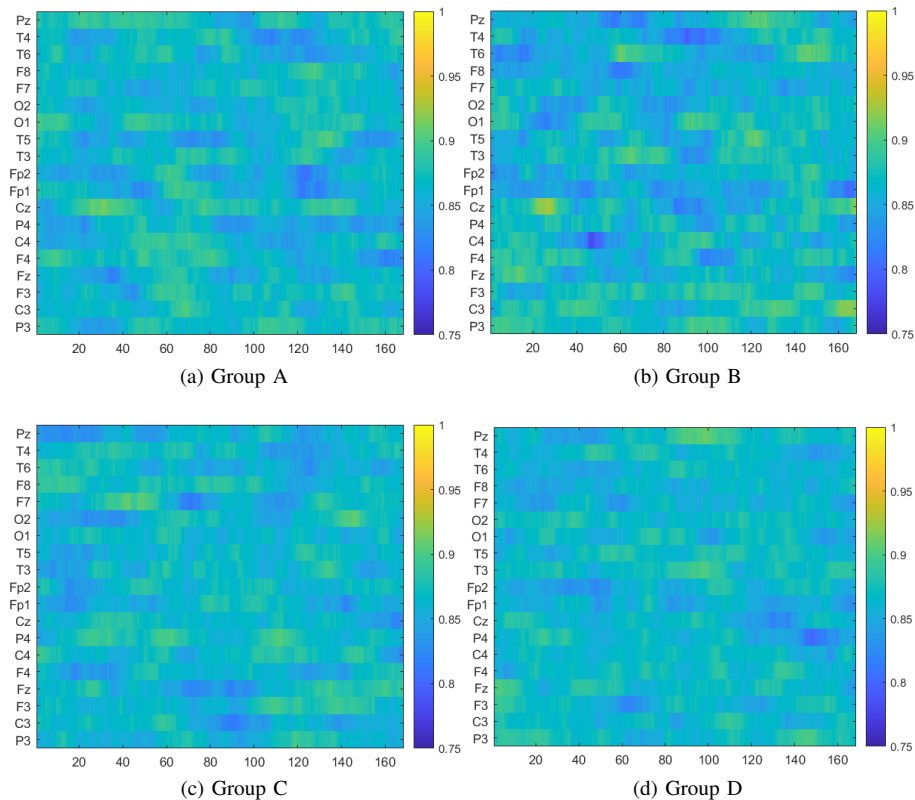


Fig. 4: Permutation entropy of resting EEG of each productivity group.

VR environment not aimed at evaluate cognition. Despite the good accuracy has been specific towards some EEG channels, the answer to why exactly it was good is absent and it is part of the well known lack of interpretability typically encountered in DL results. To address this lack of interpretability we are already focusing in two approaches that we hope it will be soon available to the scrutiny of the scientific community. One is to use nonlinear frequency domain analysis with good tracking of the parameters range (ex: power and phase) that most contribute to the best accuracy. Another course of action is the application of data driven dynamical systems methods that can also produce parameters that are might lead to a range of values indicative of good classification accuracies.

REFERENCES

- [1] J. Wang, J. Barstein, L. E. Ethridge, M. W. Mosconi, Y. Takarae, and J. A. Sweeney, "Resting state EEG abnormalities in autism spectrum disorders," *Journal of Neurodevelopmental Disorders*, vol. 5, no. 1, pp. 1–14, 2013.
- [2] B. Mazoyer, L. Zago, E. Mellet, S. Bricogne, O. Etard, O. Houdé, F. Crivello, M. Joliot, L. Petit, and N. Tzourio-Mazoyer, "Cortical networks for working memory and executive functions sustain the conscious resting state in man," Tech. Rep., 2001.
- [3] J. R. Binder, J. A. Frost, T. A. Hammeke, P. S. F. Bellgowan, S. M. Rao, and R. W. Cox, "Conceptual Processing during the Conscious Resting State: A Functional MRI Study," *Journal of cognitive neuroscience*, vol. 11, no. 1, pp. 1–14, 1999. [Online]. Available: [papers2://publication/uuid/4EB1DEEA-D766-4D1B-A36D-072AE45D2B3C](https://pubmed.ncbi.nlm.nih.gov/1072AE45D2B3C/)
- [4] M. D. Fox and M. Greicius, "Clinical applications of resting state functional connectivity," *Frontiers in Systems Neuroscience*, vol. 4, no. June, 2010.
- [5] G. M. Rojas, C. Alvarez, C. E. Montoya, M. de la Iglesia-Vayá, J. E. Cisternas, and M. Gálvez, "Study of resting-state functional connectivity networks using eeg electrodes position as seed," *Frontiers in neuroscience*, vol. 12, 235, 2018.
- [6] F. S. Racz, O. Stylianou, P. Mukli, and A. Eke, "Multifractal and entropy analysis of resting-state electroencephalography reveals spatial organization in local dynamic functional connectivity," *Scientific reports*, vol. 1-15 9(1), 2019.
- [7] F. Vecchio, C. Babiloni, R. Lizio, F. D. V. Fallani, K. Blinowska, G. Verrienti, and P. M. Rossini, "Resting state cortical eeg rhythms in alzheimer's disease: toward eeg markers for clinical applications: a review," *Supplements to Clinical neurophysiology*, vol. 62, 223-236, 2013.
- [8] R. Jacek, K. Ewa, K. Rafał, and W. Andrzej, "Resting-state eeg activity predicts frontoparietal network reconfiguration and improved attentional performance," *Scientific Reports (Nature Publisher Group)*, vol. 10(1), 2020.
- [9] A. R. Clarke, R. J. Barry, and S. Johnstone, "Resting state eeg power research in attention-deficit/hyperactivity disorder: A review update," *Clinical Neurophysiology*, 2020.
- [10] G. Li, S. Huang, W. Xu, W. Jiao, Y. Jiang, Z. Gao, and J. Zhang, "The impact of mental fatigue on brain activity: a comparative study both in resting state and task state using eeg," *BMC neuroscience*, vol. 1-9 (21), 2020.
- [11] Y. Bai, X. Xia, and X. Li, "A review of resting-state electroencephalography analysis in disorders of consciousness," *Frontiers in neurology*, vol. 8, 471, 2017.
- [12] E. Pirondini, N. Goldshuv-Ezra, N. Zinger, J. Britz, N. Soroker, L. Y. Deouell, and D. Van De Ville, "Resting-state eeg topographies: Reliable and sensitive signatures of unilateral spatial neglect," *NeuroImage: Clinical*, 2020.
- [13] A. Craik, Y. He, and J. L. Contreras-Vidal, "Deep learning for elec-

- troencephalogram (eeg) classification tasks: a review,” *Journal of neural engineering*, vol. 16(3), 2019.
- [14] Y. Roy, H. Banville, I. Albuquerque, A. Gramfort, T. H. Falk, and J. Faubert, “Deep learning-based electroencephalography analysis: a systematic review,” *Journal of neural engineering*, vol. 16(5), 2019.
- [15] C. Flexa, R. Santos, W. Gomes, and C. Sales, “A novel equidistant-scattering-based cluster index,” in *2018 7th Brazilian Conference on Intelligent Systems (BRACIS)*, Oct 2018, pp. 540–545.
- [16] J. Odom, M. Bach, M. Brigell, G. Holder, D. McCulloch, A. Tormene, and Vaegan, “Iscv standard for clinical visual evoked potentials (2009 update),” *Documenta Ophthalmologica*, vol. 120, no. 1, pp. 111–119, 2010. [Online]. Available: <http://dx.doi.org/10.1007/s10633-009-9195-4>
- [17] R. Oostenveld, P. Fries, E. Maris, and J.-M. Schoffelen, “FieldTrip: Open Source Software for Advanced Analysis of MEG, EEG, and Invasive Electrophysiological Data,” *Computational Intelligence and Neuroscience*, vol. 2011, 2011.
- [18] I. Goodfellow, Y. Bengio, and A. Courville, *Deep Learning*. MIT Press, 2016, <http://www.deeplearningbook.org>.
- [19] A. Krizhevsky, I. Sutskever, and G. E. Hinton, “Imagenet classification with deep convolutional neural networks,” in *Advances in neural information processing systems*, 2012, pp. 1097–1105. [Online]. Available: <http://papers.nips.cc/paper/4824-imagenet-classification-with-deep-convolutional-neural-networks>
- [20] S. Sra, S. Nowozin, and S. Wright, *Optimization for Machine Learning*, ser. Neural information processing series. MIT Press, 2012.
- [21] H. Yuan, C. Voelcker-Rehage, L. Huebner, and B. Godde, “Resting state eeg classification for motor learning skills using echo state networks,” 2017. [Online]. Available: <https://opus.jacobs-university.de/frontdoor/index/index/docId/759>
- [22] E. Combrisson and K. Jerbi, “Exceeding chance level by chance: The caveat of theoretical chance levels in brain signal classification and statistical assessment of decoding accuracy,” *Journal of Neuroscience Methods*, vol. 250, pp. 126 – 136, 2015, cutting-edge EEG Methods.
- [23] P. J. Allen, O. Josephs, and R. Turner, “A method for removing imaging artifact from continuous eeg recorded during functional mri,” *NeuroImage*, vol. 12, no. 2, pp. 230 – 239, 2000.
- [24] X. Jiang, G.-B. Bian, and Z. Tian, “Removal of artifacts from eeg signals: A review,” *Sensors*, vol. 19 (987), 2019.
- [25] S. Arnau, T. Möckel, G. Rinkenauer, and E. Wascher, “The interconnection of mental fatigue and aging: An EEG study,” *International Journal of Psychophysiology*, vol. 117, pp. 17–25, jul 2017.
- [26] Y. Kamikawa and T. Tanaka, “Responses in posterior parietal cortex to movement intention task with visual and tactile cues,” in *Conf Proc IEEE Eng Med Biol Soc.*, 2015, pp. 6654–6657.
- [27] R. E. Clark, “Current topics regarding the function of the medial temporal lobe memory system,” *Current Topics in Behavioral Neurosciences*, vol. 37, pp. 13–42, 2018.
- [28] M. Matulin and Mrvelj, “Fear, discomfort, and perception of time in virtual reality,” in *The 5th International Virtual Research Conference In Technical Disciplines*, 12 2018, pp. 20–24.
- [29] G. Ouyang, J. Li, X. Liu, and X. Li, “Dynamic characteristics of absence eeg recordings with multiscale permutation entropy analysis,” *Epilepsy Research*, vol. 104, no. 3, pp. 246 – 252, 2013.
- [30] C. Bandt and B. Pompe, “Permutation entropy: A natural complexity measure for time series,” *Phys. Rev. Lett.*, vol. 88, p. 174102, Apr 2002.